

## Production of $\nu_\tau$ neutrinos and $\bar{\nu}_\tau$ antineutrinos - elaborate calculation for a fixed target experiment SHiP

---

Rafał Maciuła<sup>a,\*</sup>

<sup>a</sup>*Institute of Nuclear Physics, Polish Academy of Sciences,  
ul. Radzikowskiego 152, PL-31-342 Kraków, Poland*

*E-mail:* [rafal.maciula@ifj.edu.pl](mailto:rafal.maciula@ifj.edu.pl)

We discuss cross sections for  $\nu_\tau$  and  $\bar{\nu}_\tau$  production from the direct  $D_s^\pm \rightarrow \nu_\tau/\bar{\nu}_\tau$  and chain  $D_s^\pm \rightarrow \tau^+/\tau^- \rightarrow \nu_\tau/\bar{\nu}_\tau$  decays in  $p+^{96}\text{Mo}$  scattering with proton beam  $E_{\text{lab}} = 400$  GeV *i.e.* at  $\sqrt{s_{NN}} = 27.4$  GeV. In our calculations we include  $D_s^\pm$  from charm fragmentation  $c \rightarrow D_s^+$  and  $\bar{c} \rightarrow D_s^-$  as well as those from subleading fragmentation of strange quarks/antiquarks  $s \rightarrow D_s^-$  and  $\bar{s} \rightarrow D_s^+$ . The different contributions to  $D_s^\pm$  and  $\nu_\tau/\bar{\nu}_\tau$  production rates are shown explicitly. Estimates of a number of observed  $\nu_\tau/\bar{\nu}_\tau$  in the  $\nu_\tau/\bar{\nu}_\tau + ^{208}\text{Pb}$  reaction, with 2m long target are given.

*40th International Conference on High Energy physics - ICHEP2020  
July 28 - August 6, 2020  
Prague, Czech Republic (virtual meeting)*

---

\*Speaker

## 1. Introduction

The  $\nu_\tau$  and  $\bar{\nu}_\tau$  particles were ones of last ingredients of the Standard Model discovered experimentally [1]. So far only a few  $\nu_\tau/\bar{\nu}_\tau$  neutrinos/antineutrinos were observed experimentally. Recently, it was roughly estimated that about 300 – 1000 neutrinos ( $\nu_\tau + \bar{\nu}_\tau$ ) will be observed by the SHiP (Search for Hidden Particles) experiment [2, 3]. If so then it could considerably improve our knowledge in this weakly tested corner of the Standard Model.

The  $\nu_\tau/\bar{\nu}_\tau$  neutrinos/antineutrinos are known to be primarily produced from  $D_s^\pm$  decays. The  $D_s$  mesons are abundantly produced in proton-proton collisions. Here we wish to make as realistic as possible predictions of the cross section for production of  $\nu_\tau/\bar{\nu}_\tau$  neutrinos/antineutrinos. In our model  $D_s^\pm$  mesons can be produced from both, charm and strange quark/antiquark fragmentation, with a similar probability of the transition. The  $s \rightarrow D_s$  mechanism is expected to be especially important at large rapidities (or large Feynman  $x_F$ ) [4]. Here we wish to answer whether it has consequences for forward production of neutrinos/antineutrinos for the SHiP experiment or not.

## 2. Some details of the approach

In our model we include two mechanisms of  $D_s$  meson production:  $c \rightarrow D_s^+$ ,  $\bar{c} \rightarrow D_s^-$ , called leading fragmentation, and  $\bar{s} \rightarrow D_s^+$ ,  $s \rightarrow D_s^-$ , called subleading fragmentation.

The  $c$  and  $\bar{c}$  cross sections are calculated in the collinear NLO approximation using the FONLL framework [5] or in the  $k_t$ -factorization approach [6]. Here, both the  $gg$ -fusion and  $q\bar{q}$ -annihilation production mechanisms for  $c\bar{c}$ -pairs with off-shell initial state partons are taken into consideration.

Not all charm hadrons must be created from the  $c/\bar{c}$  fragmentation. An extra hidden associated production of  $c$  and  $\bar{c}$  can occur in a complicated hadronization process. In principle,  $c$  and  $\bar{c}$  partons can also hadronize into light mesons (e.g. kaons) with non-negligible fragmentation fraction (see e.g. Ref. [7]). Similarly, fragmentation of light partons into heavy mesons may be well possible [8]. In the present study we will discuss also results of PYTHIA hadronization to  $D_s$  mesons in this context as well as our simple model of subleading fragmentation  $s \rightarrow D_s^-$  and  $\bar{s} \rightarrow D_s^+$  [4].

The  $s$  and  $\bar{s}$  distributions are calculated here in the leading-order (LO) collinear factorization approach with on-shell initial state partons and with a special treatment of minijets at low transverse momenta, as adopted e.g. in PYTHIA, by multiplying cross section by a suppression factor [9]

$$F_{sup}(p_t) = \frac{p_t^4}{((p_t^0)^2 + p_t^2)^2}. \quad (1)$$

Within this framework the cross section of course strongly depends on the free parameter  $p_t^0$  which could be, in principle, fitted to low energy charm experimental data [10]. Here, we use rather conservative value  $p_t^0 = 1.5$  GeV. We use three different sets of the collinear parton distribution functions (PDFs): the MMHT2014 [11] and the NNPDF30 [12] parametrizations. Both of them provide an asymmetric strange sea quark distributions in the proton with  $s(x) \neq \bar{s}(x)$ . The dominant partonic mechanisms are  $gs \rightarrow gs$ ,  $g\bar{s} \rightarrow g\bar{s}$  (and their symmetric counterparts) and  $gg \rightarrow s\bar{s}$ . In some numerical calculations we take into account also other  $2 \rightarrow 2$  diagrams with  $s(\bar{s})$ -quarks in the final state, however, their contributions are found to be almost negligible.

The transition from quarks to hadrons in our calculations is done within the independent parton fragmentation picture. Here, we follow the assumptions relevant for the case of low c.m.s. collision energies and/or small transverse momenta of hadrons, as discussed in our recent analysis [13], and we assume that the hadron  $H$  is emitted in the direction of parent quark/antiquark  $q$ , i.e.  $\eta_H = \eta_q$  (the same pseudorapidities or polar angles). Within this approach we set the light-cone  $z$ -scaling, i.e. we define  $p_H^+ = zp_q^+$ , where  $p^+ = E + p$ . In the numerical calculations we also include “energy conservation” conditions:  $E_H > m_H$  and  $E_H \leq E_q$ . If we take the parton as the only reservoir of energy (independent parton fragmentation) these conditions (especially the latter one) may be strongly broken in the standard fragmentation framework with constant rapidity  $y_q = y_H$  scenario, especially, when discussing small transverse momenta of hadrons. The light-cone scaling prescription reproduces the standard approach in the limit:  $m_q, m_H \rightarrow 0$ .

For  $c/\bar{c} \rightarrow D_s^\pm$  fragmentation we take the traditional Peterson fragmentation function with  $\varepsilon = 0.05$ . In contrast to the standard mechanism, the fragmentation function for  $s/\bar{s} \rightarrow D_s^\mp$  transition is completely unknown which makes the situation more difficult. For the case of light-to-light (light parton to light meson) transition rather softer fragmentation functions (peaked at smaller  $z$ -values) are supported by phenomenological studies [14]. However, the light-to-heavy fragmentation should not be significantly different than for the heavy-to-heavy case. The shape of the fragmentation function depends on mass of the hadron rather than on the mass of parton (see e.g. Ref. [8]). Therefore, here we take the same fragmentation function for the  $s/\bar{s} \rightarrow D_s^\mp$  as for the  $c/\bar{c} \rightarrow D_s^\pm$ . Besides the shape of the  $s/\bar{s} \rightarrow D_s^\mp$  fragmentation function the relevant fragmentation fraction is also unknown. The transition probability  $P = P_{s \rightarrow D_s}$  can be treated as a free parameter and needs to be extracted from experimental data. First attempt was done very recently in Ref. [4], where  $D_s^+/D_s^-$  production asymmetry was studied.

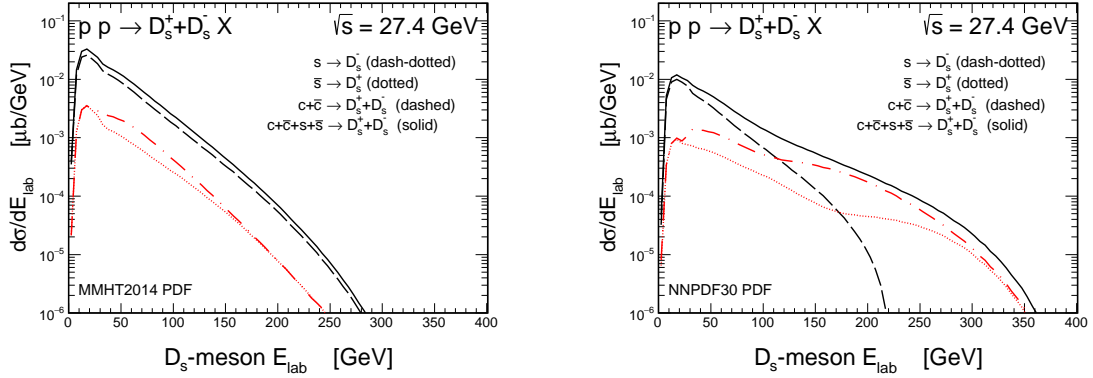


**Figure 1:** Energy distributions of  $D_s$  mesons in the laboratory frame for the MMHT2014 (left) and the NNPDF30 (right) collinear PDFs. Contributions from  $c$  and  $s$  quark fragmentation are shown separately.

In Fig. 1 we show the energy distribution of  $D_s$  mesons in the laboratory frame from proton-proton scattering at  $\sqrt{s} = 27.4$  GeV. Here we show separately the leading  $c + \bar{c} \rightarrow D_s^+ + D_s^-$  (dashed lines) and two subleading  $s \rightarrow D_s^-$  (dash-dotted lines) and  $s \rightarrow D_s^+$  (dotted lines) contributions as well as their sum  $c + \bar{c} + s + \bar{s} \rightarrow D_s^+ + D_s^-$  (solid lines). The left and right panels correspond to the MMHT2014 and the NNPDF30 PDFs, respectively. In this calculation  $P_{c \rightarrow D_s} = 0.08$  and  $P_{s \rightarrow D_s} = 0.05$  were used. A pretty much different results are obtained for the two different PDF

sets, especially for large meson energies. Depending on the collinear PDFs used our model leads to a rather small (the MMHT2014 PDF) or a fairly significant (the NNPDF30 PDF) contribution to the  $D_s$  meson production at large energies which comes from the  $s/\bar{s}$ -quark fragmentation. A future measurement of  $D_s$  mesons at low energies would help to better understand underlying mechanism and improve predictions for  $\nu_\tau/\bar{\nu}_\tau$  production for the SHiP experiment.

The considered here decay channels:  $D_s^+ \rightarrow \tau^+ \nu_\tau$  and  $D_s^- \rightarrow \tau^- \bar{\nu}_\tau$ , which are the sources of the direct neutrinos, are analogous to the standard text book cases of  $\pi^+ \rightarrow \mu^+ \nu_\mu$  and  $\pi^- \rightarrow \mu^- \bar{\nu}_\mu$  decays, discussed in detail in the past (see e.g. Ref [15]). The same formalism used for the pion decay applies also to the  $D_s$  meson decays. Since pion has spin zero it decays isotropically in its rest frame. However, the produced muons are polarized in its direction of motion which is due to the structure of weak interaction in the Standard Model. The same is true for  $D_s^\pm$  decays and polarization of  $\tau^\pm$  leptons. To calculate cross section for  $\nu_\tau/\bar{\nu}_\tau$  production the decay branching fraction  $\text{BR}(D_s^\pm \rightarrow \tau^\pm \nu_\tau/\bar{\nu}_\tau) = 0.0548 \pm 0.0023$  [16] must be included.

The  $\tau$  decays are rather complicated due to having many possible decay channels [16]. Nevertheless, all confirmed decays lead to production of  $\nu_\tau$  ( $\bar{\nu}_\tau$ ). This means total amount of neutrinos/antineutrinos produced from  $D_s$  decays into  $\tau$  lepton is equal to the amount of antineutrinos/neutrinos produced in subsequent  $\tau$  decay. But, their energy distributions will be different due to  $D_s$  production asymmetry in the case of the subleading fragmentation mechanism.

The purely leptonic channels, analogous to the  $\mu^\pm \rightarrow e^\pm (\bar{\nu}_\mu/\nu_\mu)(\nu_e/\bar{\nu}_e)$  decay cover only about 35% of all  $\tau$  lepton decays. Remaining 65% are semi-leptonic decays. They differ quite drastically from each other and each gives slightly different energy distribution for  $\nu_\tau$  ( $\bar{\nu}_\tau$ ). In our model for the decay of  $D_s$  mesons there is almost full polarization of  $\tau$  particles with respect to the direction of their motion. The mass of the  $\tau$  lepton (1.777 GeV) is very similar as the mass of the  $D_s$  meson (1.968 GeV). Therefore, direct neutrino takes away only a small fraction of energy/momentum of the mother  $D_s$ . In this calculation we use TAUOLA code [17].

In the case of the SHiP experiment a dedicated lead target was proposed. At not too small energies ( $\sqrt{s_{NN}} > 5$  GeV), the cross section for  $\nu_\tau Pb$  and  $\bar{\nu}_\tau Pb$  interactions can be obtained from elementary cross sections as:  $\sigma(\nu_\tau Pb) = Z\sigma(\nu_\tau p) + (A - Z)\sigma(\nu_\tau n)$ , and  $\sigma(\bar{\nu}_\tau Pb) = Z\sigma(\bar{\nu}_\tau p) + (A - Z)\sigma(\bar{\nu}_\tau n)$ . Shadowing effects depend on  $x$  variable (parton longitudinal momentum fraction), i.e. on neutrino/antineutrino energy. At not too high energies (not too small  $x$ ) shadowing effects are rather small and can be neglected at present accuracy having in mind other uncertainties. On the other hand for the  $x$ -ranges considered here the antishadowing and/or EMC-effect may appear non-negligible but still rather small and shall not affect the numerical predictions presented here.

The probability of interacting of neutrino with the lead target can be calculated as:

$$P_{\nu_\tau/\bar{\nu}_\tau}^{\text{target}}(E) = \int_0^d n_{\text{cen}} \sigma_{\nu_\tau Pb}(E) dz = n_{\text{cen}} \sigma_{\nu_\tau Pb}(E) d, \quad (2)$$

where  $n_{\text{cen}}$  is a number of scattering centers (lead nuclei) per volume element and the target thickness is  $d \approx 2$  m [2]. Using the NuWro Monte Carlo generator [18], we obtain  $\sigma(E)/E \sim 1.09 \times 10^{-38}$  cm<sup>2</sup>/GeV for neutrino and  $0.41 \times 10^{-38}$  cm<sup>2</sup>/GeV for antineutrino for the  $E = 100$  GeV. The number of scattering centers is  $n_{\text{cen}} = (11.340/207.2)N_A$ , where  $N_A = 6.02 \times 10^{23}$  is the Avogadro number.

The energy dependent flux of neutrinos can be written as:

$$\Phi_{\nu_\tau/\bar{\nu}_\tau}(E) = \frac{N_p}{\sigma_{pA}} d\sigma_{pA \rightarrow \nu_\tau}(E)/dE, \quad (3)$$

where  $N_p$  is integrated number of beam protons ( $N_p = 2 \times 10^{20}$  according to the current SHiP project). The  $\sigma_{pA}$  in Eq. (3) is a crucial quantity which requires a short discussion. In Ref. [3] it was taken as  $\sigma_{pA} = A \cdot \sigma_{pN}$  where  $\sigma_{pN} = 10.7$  was used. We do not know the origin of this number. Naively  $\sigma_{pN}$  should be the inelastic  $pN$  cross section.

Finally the number of  $\nu_\tau$  or  $\bar{\nu}_\tau$  observed in the  $Pb$  target is calculated from the formula:

$$N_{\nu_\tau/\bar{\nu}_\tau}^{\text{target}} = \int dE \Phi_{\nu_\tau/\bar{\nu}_\tau}(E) P_{\nu_\tau/\bar{\nu}_\tau}^{\text{target}}(E). \quad (4)$$

Here  $\Phi_{\nu_\tau/\bar{\nu}_\tau}(E)$  is calculated from different approaches to  $D_s$  meson production including their subsequent decays and  $P_{\nu_\tau/\bar{\nu}_\tau}^{\text{target}}(E)$  is obtained using Eq.(2).

### 3. Numerical results

In Fig. 2 we show the impact of the subleading contribution for the predictions of  $\nu_\tau$  and/or  $\bar{\nu}_\tau$  energy distributions for the SHiP experiment. Again we obtain two different scenarios for the two different PDF sets. The MMHT2014 PDFs set leads to an almost negligible subleading contribution in the whole energy range while the NNPDF30 PDFs set provides the subleading contribution to be dominant at larger energies ( $E_{\text{lab}} > 100$  GeV). If such distributions could be measured by the SHiP then they could be useful to constrain the PDFs in the purely known kinematical region.

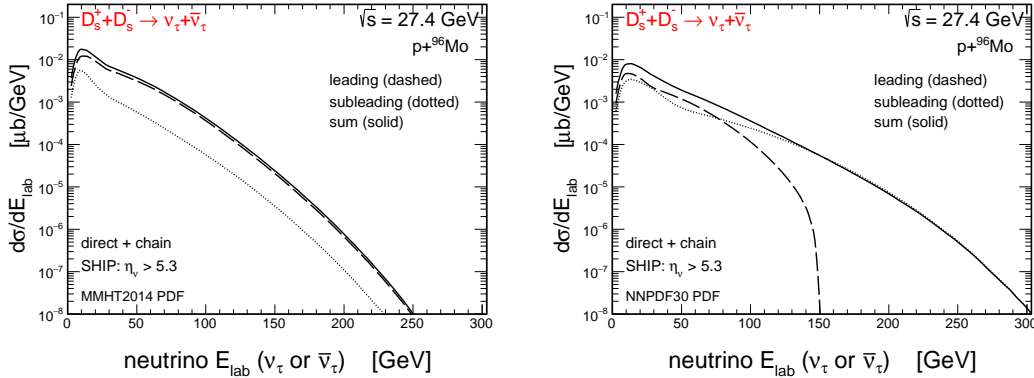


**Figure 2:** Laboratory frame energy distributions of  $\nu_\tau$  (or  $\bar{\nu}_\tau$ ) neutrinos for MMHT2014 (left) and NNPDF30 (right) sets of collinear PDFs. Here we show in the same panel the leading and subleading contributions as well as their sum.

Predictions for observed numbers of neutrinos/antineutrinos for the SHiP experiment are collected in Table 1. Quite different numbers are obtained for the different considered scenarios. We have predicted  $\sim 800$ – $2000$  tau neutrino events from charm quark fragmentation and  $\sim 200$ – $400$  tau neutrino events from strange quark fragmentation. The subleading fragmentation may increase the probability of observing  $\nu_\tau/\bar{\nu}_\tau$  neutrinos/antineutrinos. We get larger numbers than in Ref. [3]

**Table 1:** Number of observed  $\nu_\tau$  and  $\bar{\nu}_\tau$  for the SHiP experiment.

Framework/mechanism	Number of observed neutrinos				$\frac{\nu_\tau - \bar{\nu}_\tau}{\nu_\tau + \bar{\nu}_\tau}$
	flavour	direct	chain	$\nu_\tau + \bar{\nu}_\tau$	
FONLL + NNPDF30 NLO PDF $c/\bar{c} \rightarrow D_s^\pm \rightarrow \nu_\tau/\bar{\nu}_\tau$	$\frac{\nu_\tau}{\bar{\nu}_\tau}$	96 27	515 180	818	0.49
LO coll. + NNPDF30 LO PDF $s/\bar{s} \rightarrow D_s^\pm \rightarrow \nu_\tau/\bar{\nu}_\tau$	$\frac{\nu_\tau}{\bar{\nu}_\tau}$	93 75	1092 156	1416	0.67
FONLL + MMHT2014nlo PDF $c/\bar{c} \rightarrow D_s^\pm \rightarrow \nu_\tau/\bar{\nu}_\tau$	$\frac{\nu_\tau}{\bar{\nu}_\tau}$	277 80	1427 508	2292	0.49
LO coll. + MMHT2014lo PDF $s/\bar{s} \rightarrow D_s^\pm \rightarrow \nu_\tau/\bar{\nu}_\tau$	$\frac{\nu_\tau}{\bar{\nu}_\tau}$	59 21	435 117	632	0.56

but smaller than in Ref. [2]. The chain contribution is significantly larger (about factor 7) than the direct one. For the MMHT2014 distribution the contribution of the leading mechanism is much larger than for the subleading one. For the NNPDF30 distributions the situation is reversed. We predict large observation asymmetry (see the last column) for  $\nu_\tau$  and  $\bar{\nu}_\tau$ . This asymmetry is bigger than shown e.g. in Refs. [2, 3]. This is due to the subleading mechanism for  $D_s^\pm$  meson production included in the present paper. The observation asymmetry for the leading contribution which comes from the differences of the  $\nu_\tau$  and  $\bar{\nu}_\tau$  interactions with target are estimated at the level of 50%. In the case of the subleading contribution the asymmetry increases to 60-70%. More details of the study can be found in original article [19].

## References

- [1] K. Kodama *et al.* [DONUT Collaboration], Phys. Lett. B **504**, 218 (2001).
- [2] A. Buonaura [SHiP Collaboration], PoS DIS **2016**, 260 (2016).
- [3] W. Bai and M. H. Reno, J. High Energy Phys. **02**, 077 (2019).
- [4] V. P. Goncalves, R. Maciuła and A. Szczurek, Phys. Lett. B **794**, 29 (2019).
- [5] M. Cacciari, M. Greco and P. Nason, J. High Energy Phys. **05** (1998) 007.
- [6] S. Catani, M. Ciafaloni and F. Hautmann, Phys. Lett. B **242** (1990) 97.
- [7] M. Epele, C. García Canal and R. Sassot, Phys. Lett. B **790**, 102 (2019).
- [8] T. Kneesch, B. A. Kniehl, G. Kramer and I. Schienbein, Nucl. Phys. B **799**, 34 (2008).
- [9] T. Sjöstrand *et al.*, Comput. Phys. Commun. **191**, 159 (2015).
- [10] R. Maciuła and A. Szczurek, Phys. Rev. D **97**, no. 7, 074001 (2018).
- [11] L. A. Harland-Lang *et al.*, Eur. Phys. J. C **75**, no. 5, 204 (2015).
- [12] R. D. Ball *et al.* [NNPDF Collaboration], J. High Energy Phys. **04**, 040 (2015).
- [13] R. Maciuła and A. Szczurek, arXiv:1907.13388 [hep-ph].
- [14] V. Bertone *et al.* [NNPDF Collaboration], Eur. Phys. J. C **77**, no. 8, 516 (2017).
- [15] P. Renton, Cambridge, UK: Univ. Pr. (1990) 596 p
- [16] M. Tanabashi *et al.* [Particle Data Group], Phys. Rev. D **98**, no. 3, 030001 (2018).
- [17] S. Jadach, J. H. Kuhn and Z. Wąs, Comput. Phys. Commun. **64**, 275 (1990).
- [18] J. Żmuda *et al.*, Acta Phys. Polon. B **46**, no. 11, 2329 (2015).
- [19] R. Maciuła, A. Szczurek, J. Zaremba and I. Babiarez, J. High Energy Phys. **01**, 116 (2020).